Supplementary Information (SI)

Porous Reduced Graphene Oxide (rGO)/WO_3 Nanocomposites for the Enhanced Detection of NH_3 at Room Temperature

G. Jeevitha[a], R. Abhinayaa[a], D. Mangalaraj[a*], N. Ponpandian[a], P. Meena[b], Veena Mounasamy[c] and Sridharan Madanagurusamy[c]

[a] Department of Nanoscience and Technology, Bharathiar University, Coimbatore 641 046, India.

[b] Department of Physics, PSGR Krishnammal College for Women, Coimbatore 641 004, India

[c] Functional Nanomaterials & Devices Laboratory, Centre for Nanotechnology & Advanced Biomaterials and School of Electrical & Electronics Engineering, Shanmugha Arts, Science, Technology and Research Academy (SASTRA), Thanjavur - 613 401, India

*Corresponding author. E-mail address: dmraj800@yahoo.com (D. Mangalaraj)

ST:1 Existing literature for WO_3 nanostructures towards NH_3 sensing

Material	Preparation method	Morphology	Concentration	Response	Working Temperature	Ref
Pure WO_3, Au, Pt and Pd-doped WO_3	Sol–gel process	---	400 - 4000 ppm	WO_3 = 1.3 and Pt-doped WO_3 =12	250 - 450 °C	[1]
Pure WO_3, Pt-doped WO_3	Acidic precipitation route	Nanoparticles	100 - 4000 ppm	WO_3 = 9 and Pt-doped WO_3 = 125	350 °C	[2]
Pure WO_3 and Pt-	Nanocasting method	Mesoporous	50 - 1500 ppm	WO_3 = 6.72 Pt-loaded	125 - 200 °C	[3]

loaded WO_3				WO_3 = 13.6		
Chromium-doped WO_3	Reflux condensation process	Nanoparticles	500 ppm	WO_3:Cr = ~ 82	700 °C	[4]
WO_3	Thermal oxidation process	Nanowire	1500 ppm	WO_3 = 9.7	250 °C	[5]
Pure WO_3, Cr and Pt-doped WO_3	Self-assembly and Sol-gel process	Macroporous	6.2-74 ppm	WO_3 = 3.3 Pt-doped WO_3 =110	225 °C	[6]
WO_3	Acid precipitation method	Nanorods	50 - 200 ppm	96%	400 °C	[7]
$W_{18}O_{49}$	Solvothermal technique	Nanowires	0.1-10 ppm	---	Room temperature	[8]
Polypyrrole -WO_3	Electrospinning	Nanofibers	1-20 ppm	27%	100 °C	[9]
WO_3	Electrospinning	Nanofibers	50-500 ppm	---	350 °C	[10]
WO_3 and Cr–WO_3	Sol–gel process	------	50 - 500 ppm	---	250 °C	[11]
WO_3	Hydrothermal synthesis	Nanorods	25-250 ppm	192	50 °C	[12]

2.1. Synthesis of WO_3 nanostructures

The chemicals purchased from Sigma Aldrich and Hi-media are of analytical grade, and used without further purification. The facile solvothermal method was used to synthesize the different morphologies; WO_3 Aggregated nanoparticle (WO_3-1), WO_3 nanospheres (WO_3-2) and WO_3 nanorods (WO_3-3) nanostructures were obtained on changing the surfactant. A typical synthesis process was as follows: Initially 0.1 M of

WCl_6 was dissolved in 30 mL of ethanol and 0.05 M of sodium dodecyl sulfate (SDS) was dissolved in 30 mL ethanol. Both the solutions were stirred separately for 1 hour. The SDS solution was then added dropwise into the WCl_6 solution, which was dark blue in colour. The mixture was stirred for another hour at room temperature, and then shifted into a teflon-lined stainless-steel autoclave and kept at 180˚C for 12 h. The resultant product was washed with double distilled water and ethanol to remove the unreacted ions by centrifugation before drying at 65 ˚C for 24 h. The final product obtained, $WO_3.H_2O$ was calcined at 450 ˚C for 3 h to remove water molecules and to achieve pristine WO_3, named as WO_3-1. For the preparation of WO_3-2 and WO_3-3, the surfactant was changed to hexamethylenetetramine (HMTA) and cetyltrimethyl ammonium bromide (CTAB) respectively. The detailed parameters for the synthesis of WO_3 nanostructures are summarized in ST2 and the scheme for the preparation of WO_3 is given in Fig. S1.

ST2: Synthesis parameters for the preparation of WO_3 nanostructures.

Samples	Tungsten source	Solvent used	pH	Surfactant used	Temperature and time	Annealing temperature	Morphology
WO_3-1	WCl_6	Ethanol	0.5	SDS	180 ˚C, 12 h	450 ˚C, 3 h	Aggregated nanoparticles
WO_3-2	WCl_6	Ethanol	0.5	HMTA	180 ˚C, 12 h	450 ˚C, 3 h	Nanospheres
WO_3-3	WCl_6	Ethanol	0.5	CTAB	180 ˚C, 12 h	450 ˚C, 3 h	Nanorods

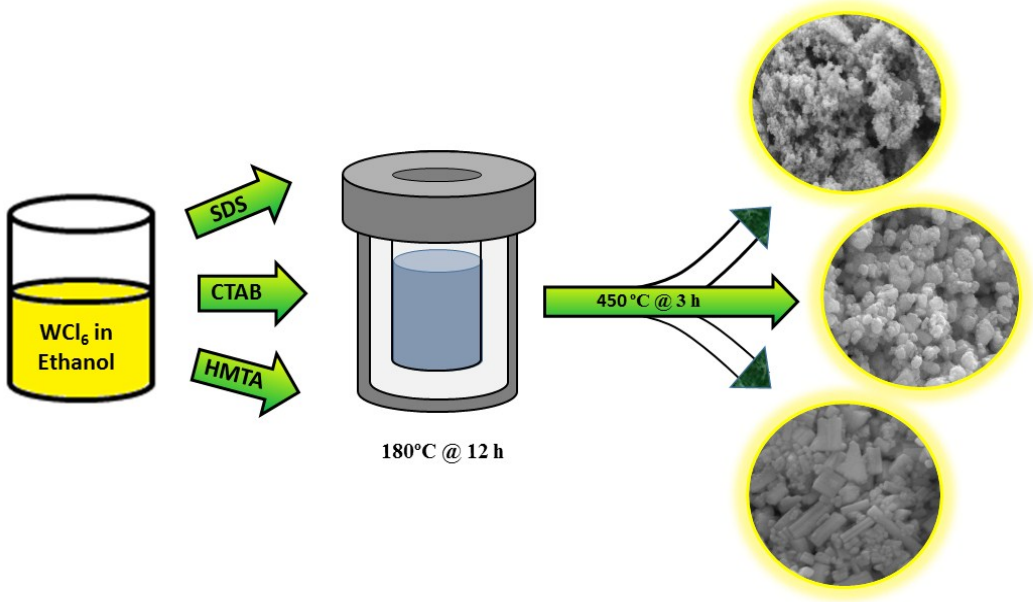

Fig. S1 Schematic diagram for the preparation of WO_3 nanostructures with three different surfactants.

XRD

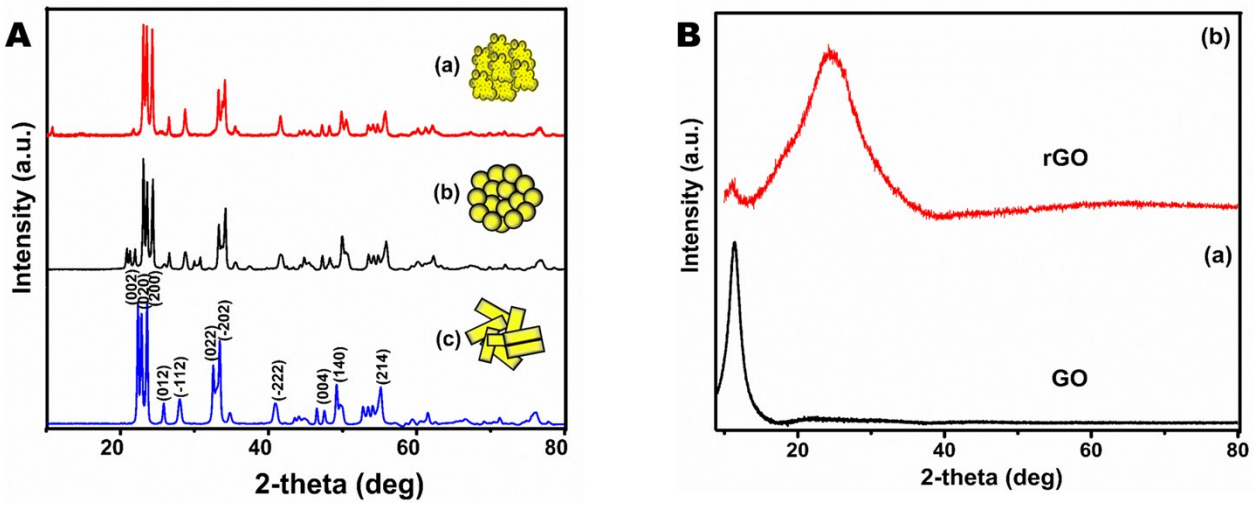

Fig. S2 Powder XRD spectrum of different morphologies of WO_3 nanostructures obtained by solvothermal method using different surfactants (a) WO_3-1 (b) WO_3-2 and (c) WO_3-3

RAMAN

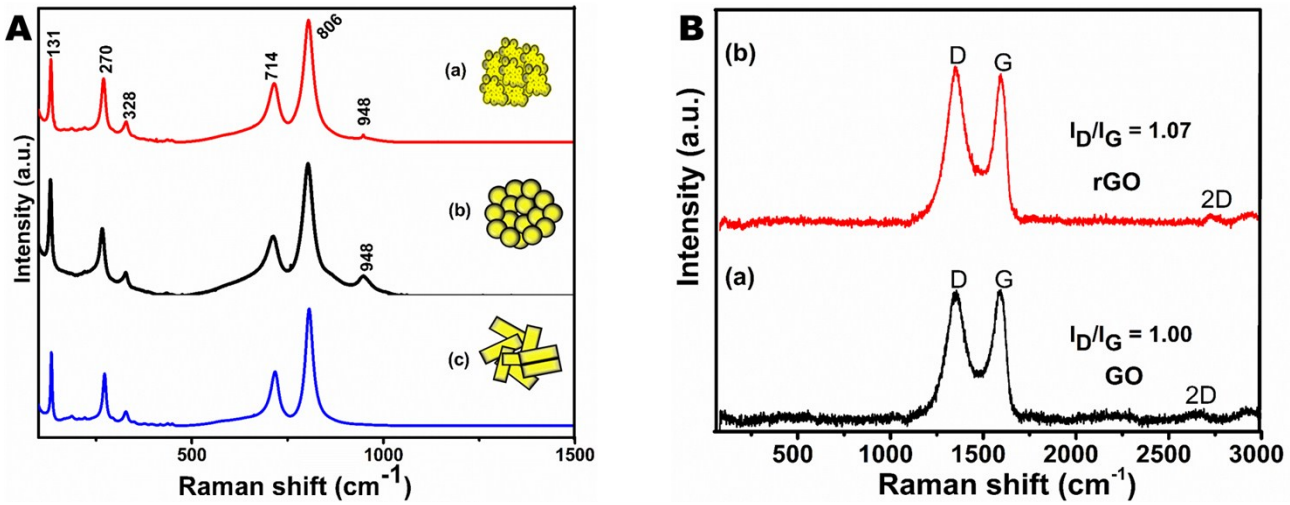

Fig. S3 Raman Spectrum of WO_3 nanostructures for different morphologies (a) WO_3-1 (b) WO_3-2 (c) WO_3-3

For all the WO_3 crystalline phases, three main frequency regions are observed; the first in the low frequency region (<200 cm^{-1}), where several peaks associated with the lattice modes appear; the second at intermediate frequencies (200–400 cm^{-1}) showing O–W–O bending mode, and the third at higher frequencies (600–900 cm^{-1}) with the peaks associated with W–O stretching modes. Sharp peaks appear at 132, 272, 328,714 and 806 cm^{-1} and these peaks confirm the WO_3 formation with a monoclinic structure [13]. From the Raman spectra, it is clear that all the samples have the same monoclinic phase of WO_3 irrespective of the different morphologies.

FESEM:

Three different morphologies of WO_3 have been prepared using the three surfactants SDS, HMTA and CTAB, where SDS is an anionic surfactant, CTAB is cationic and HMTA cationic. When the SDS is introduced into the prepared precursor solution, SDS molecules get adsorbed on the surface of WCl_6 as tiny particles. These tiny particles mold into different shapes of WO_3 nuclei, which grow into the nanoparticles when subjected to hydrothermal treatment. Fig. S4 (a and b) shows the observed FESEM images for the SDS assisted sample, which has a cloud like morphology. This sample exhibits a particle size distribution of 125-130 nm. Fig. S4 (c and d) shows the FESEM images for the HMTA assisted sample. Well-defined nanospheres

are observed, with diameters in the range of 110-120 nm. From Fig. S4 (e and f), it is evident that the presence of CTAB is favorable for the formation of WO_3 nanorods. In general, CTAB is a cationic surfactant, which could pave the way for self-assembly and the formation WO_3 1D nanorods and the average particle size is found to be between 110 - 120 nm [14-16].

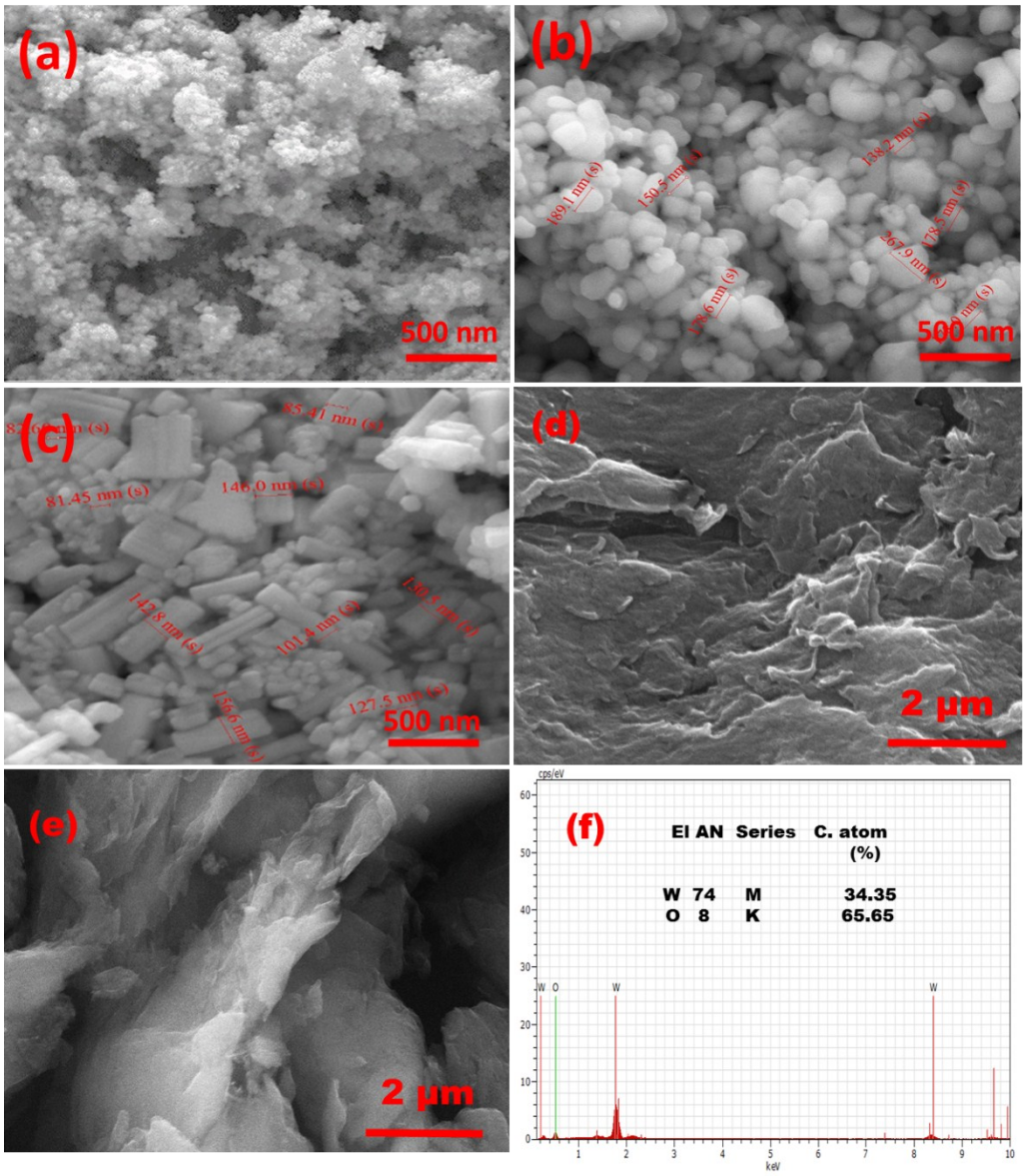

Fig. S4 FESEM image of WO_3 synthesized using different surfactants and their morphologies (a) WO_3-1 aggregated nanoparticles (SDS as surfactant) (b) WO_3-2 nanospheres (HMTA as surfactant) (c) WO_3-3 nanorods (CTAB as surfactant) (d) graphene oxide sheet (e)Reduced Graphene Oxide and (f) EDAX spectrum of rGO/WO_3

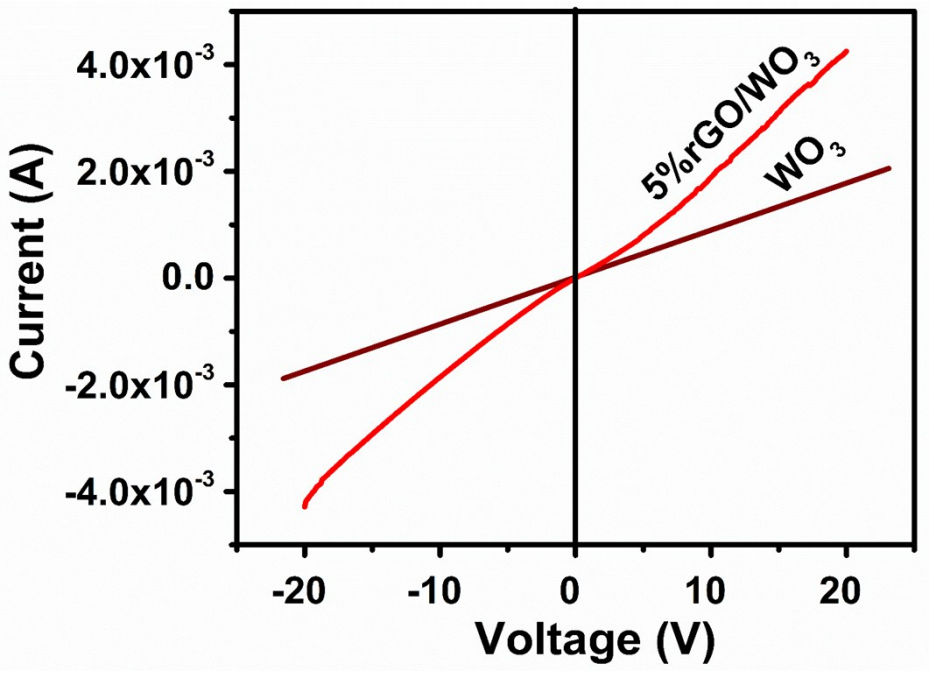

Fig. S5: I-V characteristics of WO_3 nanospheres and 5% rGO/WO_3 nanocomposite

Gas sensing

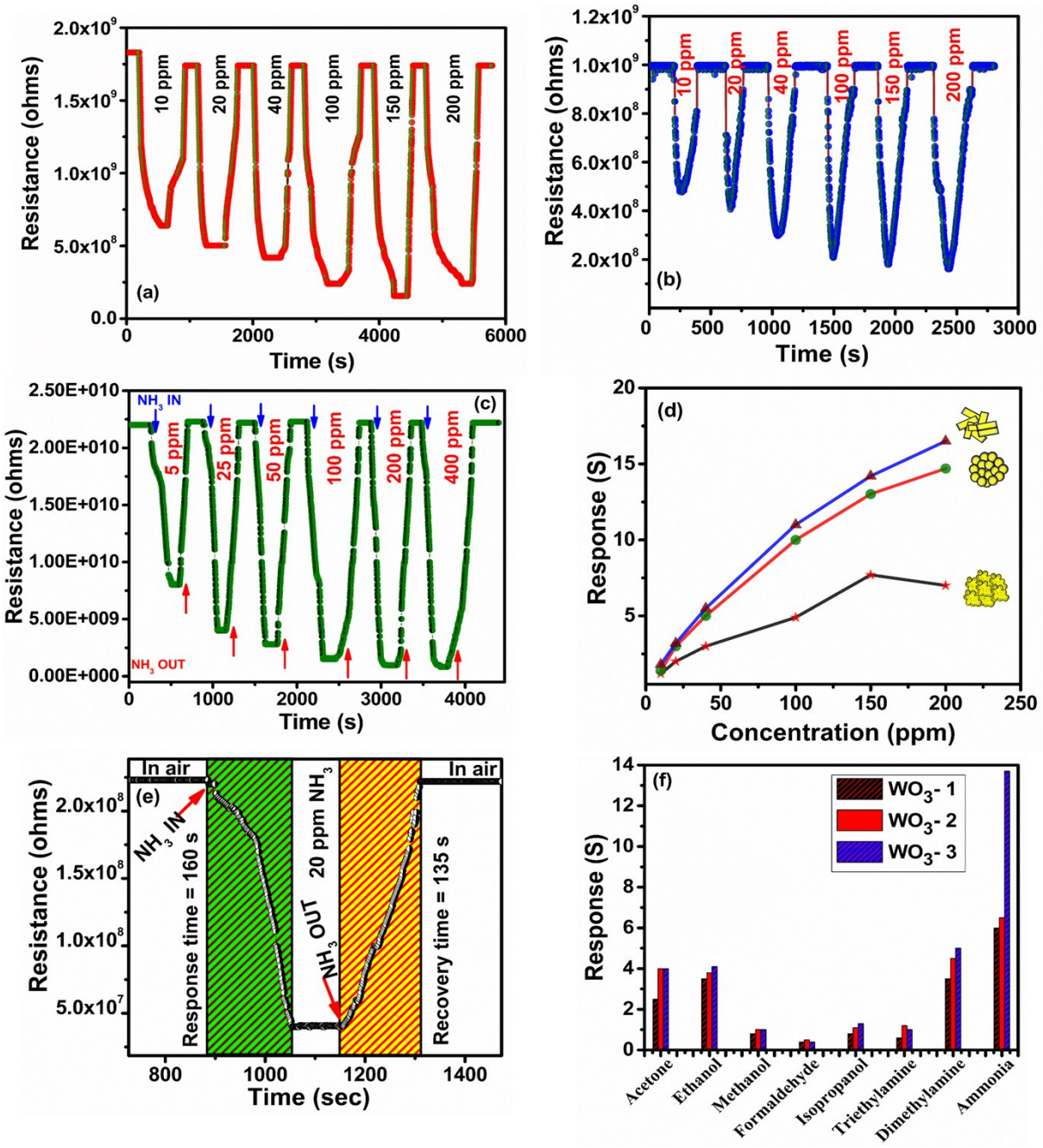

Fig. S6: Dynamic response, sensitivity and selectivity graph of WO_3 nanostructures (a) WO_3-1 aggregated nanoparticles (SDS as surfactant) (b) WO_3-2 nanospheres (HMTA as surfactant) (c) WO_3-3 nanorods (d) Sensor response towards different morphologies (e) Response and recovery time of WO_3-3 nanorods towards 20 ppm NH_3 and (f) Selectivity of different morphologies WO_3 nanostructures.

ST3: Comparison on the responses of different nanomaterials with graphene and PANI towards NH_3 sensing

S.No	Materials	Concentration	Temperature	Sensor response	Res/Rec time	Ref
1	Graphene-Polyaniline hybrid	10-100 ppm	Room temperature (22.0 °C)	344.2	20/27	[17]
2	rGO−SnO_2 films	25 -2800 ppm	Room temperature	1.3-22.0	210/150	[18]
3	SnO_2–WO_3 bilayer thin film	50–1000 ppm NH_3	300 °C	7.1	1.9–20.3	[19]
4	PANI/WO_3	10 ppm	Room temperature	20.1	13/ 49 s	[20]
5	Tinoxide-polyaniline nanocomposite	100–500 ppm	Room temperature	9-15%	15/80 s (300 ppm)	[21]
6	rGO/WS_2 heterojunctions	10 – 50 ppm	Room temperature	121-256%	~60/300 s (10 ppm)	[22]
7	Graphene-Based Wearable Gas Sensors	ppt - ppm	Room temperature and temperature dependent	---	-----	[23]
8	rGO	300 ppm	Room Temperature	3.1%	~45/85 s	[24]
9	WO_3 nanostructures (aggregated nanoparticles,	**10-200 ppm**	**Room**	1.2-7, 1.4-14.7 & 1.8-16.0	~160/135 s for nanorod	This work

	nanospheres and nanorods)		**temperature**			
10.	**WO_3/rGO nanocomposite**	**10-100 ppm**	**Room temperature**	**4.50-15.8**	**18-24 s (40 ppm)**	**This work**

References

[1] V. Srivastava and K. Jain, highly sensitive NH_3 sensor using Pt catalyzed silica coating over WO_3 thick films, *Sensors and Actuators B,* 133 (2008) 46–52.

[2] T.D. Senguttuvana, V. Srivastava, J. S. Tawal, M. Mishraa, S. Srivastava, K. Jain, Gas sensing properties of nanocrystalline tungsten oxide synthesized by acid precipitation method, *Sensors and Actuators B,* 150 (2010) 384–388.

[3] Y. Wang, J. Liu, X. Cui, Y. Gao, J. Ma, Y. Sun, P. Sun, F. Liu, X. Liang, T. Zhang, G. Lu, NH_3 gas sensing performance enhanced by Pt-loaded on mesoporous WO_3, *Sensors and Actuators B*, 238 (2017) 473–481.

[4] I. Jimenez, M. A. Centeno, R. Scotti, F. Morazzoni, J. Arbiol, A. Corneta and J. R. Morantea, *J. Mater. Chem.,* 14 (2004) 2412 – 2420.

[5] N.V. Hieu, V. V. Quang, N. D. Hoa, D, Kim, Preparing large-scale WO_3 nanowire-like structure for high sensitivity NH_3 gas sensor through a simple route, *Current Applied Physics.,* 11 (2011) 657-661.

[6] M. D'Arienzo, L. Armelao, C. M. Mari, S. Polizzi, R. Ruffo, R. Scotti, and F. Morazzoni., Macroporous WO_3 Thin Films Active in NH_3 Sensing: Role of the Hosted Cr Isolated Centers and Pt Nanoclusters, *J. Am. Chem. Soc.*, 133 (2011) 5296 -5304.

[7] L. Wang, J. Pfeifer, C. Balázsi, and P. I. Gouma, Synthesis and Sensing Properties to NH_3 of Hexagonal WO_3 Metastable Nanopowders, *Materials and Manufacturing Processes.*, 22 (2007) 773-776.

[8] Y.M. Zhao, Y.Q. Zhu, Room temperature ammonia sensing properties of $W_{18}O_{49}$ nanowires, *Sensors and Actuators B.,* 137 (2009) 27-31.

[9] T. A. Ho, T.S. Jun, Y. S. Kim, Material and NH_3-sensing properties of polypyrrole-coated tungsten oxide nanofibers, *Sensors and Actuators B,* 185 (2013) 523–529.

[10] G. Wang, Y. Ji, X. Huang. X. Yang, P. I. Gouma, and M. Dudley, Fabrication and Characterization of Polycrystalline WO_3 Nanofibers and Their Application for Ammonia Sensing, *J. Phys. Chem. B,* 110 (2006) 23777-23782.

[11] M. Epifani, N. G. Castelloe, J. D. Prades, A. Cirera, T. Andreu, J. Arbiol, P. Sicilianoa, J. R. Morante, Suppression of the NO_2 interference by chromium addition in WO_3-based ammonia sensors. Investigation of the structural properties and of the related sensing pathways, *Sensors and Actuators B,* 187 (2013) 308–312.

[12] D. D. Nguyen, D. V. Dang and D. C. Nguyen, Hydrothermal synthesis and NH_3 gas sensing property of WO_3 nanorods at low temperature, *Adv. Nat. Sci.: Nanosci. Nanotechnol*., 6 (2015) 035006.13

[13] S. Poongodi, P. S. Kumar, Y. Masuda, D. Mangalaraj, N. Ponpandian, C. Viswanathan and S. Ramakrishna, Synthesis of hierarchical WO_3 nanostructured thin films with enhanced electrochromic performance for switchable smart windows*, RSC Adv.,* 5 (2015) 96416-96427.

[14] N. Asim, S. Radiman & M. A. B. Yarmo, Synthesis of WO_3 in nanoscale with the usage of sucrose ester microemulsion and CTAB micelle solution, *Materials Letters*, *6* (2007) 2652-2657.

[15] Y. X. Wang, J. Sun, X. Y. Fan and X. Yu, A CTAB-assisted hydrothermal and solvothermal synthesis of ZnO nanopowders, *Ceramics International*, 37 (2011) 3431–3436.

[16] G. Bailly, J. Rossignol, B. de Fonseca, P. Pribetich, and D. Stuerga, Microwave Gas Sensing with Hematite: Shape Effect on Ammonia Detection Using Pseudocubic, Rhombohedral, and Spindlelike Particles, *ACS Sens*., 1 (2016) 656−662.

[17] S. Bai, Y. Zhao, J. Sun, Y. Tian, R. Luo, D. Li and A. Chen, *Chem. Commun.,* 2015, 51, 7524 DOI: 10.1039/C5CC01241D

[18] R. Ghosh, A. K. Nayak, S. Santra, D. Pradhan and P. K. Guha, Enhanced Ammonia Sensing at Room Temperature with Reduced Graphene Oxide/ Tin Oxide Hybrid Film, *RSC Adv.,* 5(62) (2015), 50165-50173, DOI: 10.1039/C5RA06696D.

[19] N. V. Toan, C. M. Hung, N. V. Duy, N. D. Hoa, D. T.T. Le, N. V. Hieu, Bilayer SnO_2–WO_3 nanofilms for enhanced NH_3 gas sensing performance, *Materials Science & Engineering B*, 224 (2017) 163–170

[20] S. Li, P. Lin, L. Zhao, C. Wang, D. Liu, F. Liu∗, P. Sun, X. Liang, F. Liu, X. Yan, Y. Gao, G. Lu, The room temperature gas sensor based on Polyaniline@flower-likeWO_3 nanocomposites and flexible PET substrate for NH_3 detection*, Sensors and Actuators B,* 259 (2018) 505–513

[21] N.G. Deshpandea, Y.G. Gudage, Ramphal Sharma, J.C. Vyas, J.B. Kim, Y.P. Lee, Studies on tin oxide-intercalated polyaniline nanocomposite for ammonia gas sensing applications, *Sensors and Actuators B,* 138 (2009) 76–84

[22] X. Wang, D. Gu, X Li, S. Lin, S. Zhao, M. N. Rumyantseva, A. M. Gaskov, Reduced graphene oxide hybridized with WS_2 nanoflakes based heterojunctions for selective ammonia sensors at room temperature, *Sensors and Actuators B: Chemical*, 282 (2019) 290-299.

[23] Eric Singh, M. Meyyappan, and Hari Singh Nalwa, Flexible Graphene-Based Wearable Gas and Chemical Sensors, ACS Appl. Mater. Interfaces, 9(2017) 34544−34586.

[24] Cherukutty Ramakrishnan Minitha, Velunair Sukumaran Anithaa, Vijayakumar Subramaniam and Ramasamy Thangavelu Rajendra Kumar, Impact of Oxygen Functional Groups on Reduced Graphene Oxide Based Sensors for Ammonia and Toluene Detection at Room Temperature, ACS Omega, 3 (2018) 4105−4112